PHYSICS AND CHEMISTRY OF SOLID STATE
V. 25, No. 4 (2024) pp. 764-772
Section: Physics

DOI: 10.15330/pcss.25.4.764-772

Vasyl Stefanyk Precarpathian National University

ФІЗИКА І ХІМІЯ ТВЕРДОГО ТІЛА
Т. 25, № 4 (2024) С. 764-772
Фізико-математичні науки

PACS: 73.50.Pz; 71.15.Ap

ISSN 1729-4428 (Print)
ISSN 2309-8589 (Online)

J. Adeyemi Owolabi[1], H. Ali[1], Ukorah N. Ijeoma[1], M.Y. Onimisi[1], R.A. Tafida[1], J. Olalekan Awujoola[2], Hassan Gambo[1]

Investigating the performance of Tin-based perovskite solar cell with Cadmium Sulphide as etm and graphene as htm using SCAPS-1D

[1]*Department of Physics Nigerian Defence Academy, Kaduna, Nigeria, jaowolabi@nda.edu.ng*
[2]*Directorate of information and communication Technology NDA Kaduna, Kaduna, Nigeria*

Solar cells based on lead-free perovskite have demonstrated great potential for renewable energy. The SCAPS-1D simulation software was used in this study to perform device modelling of a lead-free perovskite solar cell of the architecture Glass/FTO/CdS/$CH_3NH_3SnI_3$/Graphene/Pt. For the performance evaluation, an optimization process of the different parameters such as thickness of the ETM, Absorber, Bandgap energy of the hole transport material was conducted. Extensive discussion on its effect on the performance of the solar cell parameters were stated. An optimal ETM and Absorber layer thickness was achieved at 40nm and 950nm. The Bandgap energy gave an optimal performance of device parameters at 0.9eV. Temperature variations were simulated and it was noted that the device had a minimal decrease in PSC parameters performance with increasing temperature. The final optimized device structure achieved a PCE, Voc, Jsc and FF of 25.65%, 0.9606 V, 33.2491(mA/cm^2), and 80.32% respectively. Therefore, we expect that our findings will pave the way for the development of lead-free and highly effective perovskite solar cells.

Keywords: Hole Transport Layer; Electron Transport Layer; SCAPS-1D.

Received 02 July 2024; Accepted 01 November 2024.

Introduction

As we confront the pressing challenges of climate change and diminishing fossil fuel reserves, the imperative for clean and sustainable energy sources has reached unprecedented urgency. Solar energy, leveraging the abundant power of the sun, emerges as a beacon of hope in this endeavor [1,2]. In stark contrast to conventional energy sources that emit harmful greenhouse gases, solar energy stands as a renewable resource capable of generating electricity without polluting the environment. This introduction explores the manifold advantages of solar energy and investigates the promising potential of tin-based perovskite solar cells, a groundbreaking technology poised to propel solar energy to new heights. Solar energy offers a plethora of benefits that underscore its viability as a cornerstone of a sustainable future. The sun's energy is virtually limitless, in stark contrast to fossil fuels, which are finite resources requiring millions of years to replenish. This ensures a reliable and enduring source of power for generations to come [3,4]. Solar energy production does not entail combustion or the release of harmful pollutants such as greenhouse gases, sulfur oxides, or nitrogen oxides. This notable characteristic significantly mitigates our carbon footprint and contributes to the global effort to combat climate change [5]. Solar energy can be harnessed across various scales, ranging from large-scale solar farms supplying electricity to entire grids to rooftop solar panels powering individual residences. This versatility renders it a suitable solution for both centralized and decentralized energy production, thereby enhancing energy resilience and accessibility [6]. Once installed, solar panels necessitate minimal ongoing maintenance, boasting lifespans of 25 years or more. This translates to substantial cost savings compared to traditional energy sources, which entail constant fuel replenishment and maintenance expenditures [7]. The solar industry is experiencing rapid

expansion, fostering job creation and bolstering the green economy. Furthermore, as solar technology continues to advance, it becomes increasingly cost-competitive with conventional sources, rendering it a more appealing option for consumers [8]. While silicon-based solar cells have long reigned supreme in the realm of photovoltaics, a rising contender has emerged: tin-based perovskite solar cells. Perovskites, a class of materials distinguished by their unique crystal structure, exhibit exceptional light-harvesting capabilities [9]. Though still in the developmental stage, tin-based perovskite cells have demonstrated efficiencies surpassing 14%, showcasing substantial potential to rival or even outperform traditional silicon cells [10]. Perovskites can be synthesized via simpler and less energy-intensive processes relative to silicon, potentially leading to decreased production expenses [11]. As of today, the power conversion efficiency (PCE) of PSCs has improved from 3.1% to 25.7% for single-junction cells, and up to 31.3% for tandem architectures [12, 13]. PSCs produced using solution-based chemical processes have shown promising PCE levels with cost advantages [14], making them a competitive alternative to traditional silicon solar cells. Tin-based perovskite cells can be deposited onto lightweight and flexible substrates, opening avenues for novel applications in building-integrated photovoltaics and portable power solutions [15]. The advancement of tin-based perovskite solar cells signifies a significant stride forward in photovoltaic technology. While challenges pertaining to long-term stability and large-scale manufacturing necessitate further attention, the prospective benefits of this technology are unequivocal. As ongoing research refines tin-based perovskites, they are poised to exert a transformative influence on the future of solar energy, enabling more efficient and sustainable harnessing of the sun's power.

I. Device structure and simulation methology

The cell model used for this simulation in Fig.1 describes the structure of the perovskites based on FTO/ETM/$CH_3NH_3SnI_3$/HTM/Pt which consists of transparent conducting oxide, the electron transport material, methyl ammonium tin tri-iodide, the hole transport material (Graphene) and the metal back contact Platinum. The electron transporting materials (ETMs) consist of Cadmium Sulphide (CdS). The cell was illuminated through transparent conductive oxide (FTO), which serves as a window layer and passes across the electron transport layer (CdS), which serves as a buffer layer and enters the absorber layer to the hole transport material.

1.2. SCAPS-1D Basic Semiconductor Equation

SCAPS-1D simulator was developed by Marc Burgelman *et al* in 2000 [16] to simulate the electrical characteristics i.e. simulating alternating current and direct current electrical attributes of thin-film hetero-junction solar cells. SCAPS-1D is a one-dimensional solar cell simulation program based on three coupled differential equations by solving the basic semiconductor equations such as Poisson equation, continuity of electrons and holes [17]. SCAPS analyses the physics model in PSCs and it explains the recombination profiles, electric field distribution, carrier transport mechanism and individual current densities. Poisson's equation can be given by:

$$\frac{d}{dx}\left[-\varepsilon(x)\frac{d\emptyset}{dx}\right]= q[p(x) - n(x) + N_D^+(x) - N_A^-(x) + p_t(x) - n_t(x)] \quad (1b)$$

where $\emptyset$ is the electrostatic potential, q is the charge, ε is the dielectric constant of the medium, p is the free hole density, n is the free electron density, N_D^+ is the ionized-donor density,

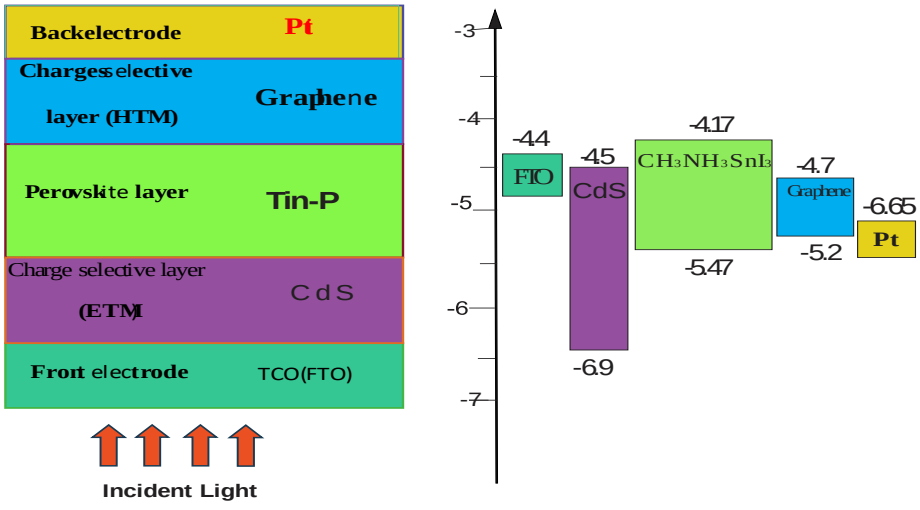

Fig. 1. Device architecture of the Tin-based perovskite solar cell and Energy band alignment for the proposed device.

N_A^- is the $\frac{d^2\phi_{(x)}}{dx^2} = \frac{q}{\varepsilon}[p(x) - n(x) + N_D^+(x) - N_A^-(x) + p_t(x) - n_t(x)]$. (1a)

ionized-acceptor density, n_t and p_t are trapped electrons density and trapped hole density respectively.

The continuity equations of electrons can be described by:

$$q\frac{\partial n(x,t)}{\partial t} = \frac{\partial J_n}{\partial x} + qG_n(x,t) - qR_n(x,t). \quad (2a)$$

$$\frac{\partial n(x,t)}{\partial t} = \frac{1}{q}\frac{\partial J_n}{\partial x} + G_n(x,t) - R_n(x,t). \quad (2b)$$

Where J_n is the electron current density, G is the generation rate, R is the recombination rate.

The continuity equations of holes can be described by:

$$q\frac{\partial P(x,t)}{\partial t} = -\frac{\partial J_P}{\partial x} + qG_P(x,t) - qR_P(x,t) \quad .(3a)$$

$$\frac{\partial P(x,t)}{\partial t} = -\frac{1}{q}\frac{\partial J_P}{\partial x} + G_P(x,t) - R_P(x,t) \quad .(3b)$$

where J_P is the hole current density.

1.3. Basic Parameters

The basic material parameters are meticulously chosen, drawing from a blend of experimental data and theoretical findings. The FTO, CdS (ETM) absorber layer parameters are referenced from [18, 19]. The HTM layer, primarily composed of Graphene, is cited from Gagandeep et al., 2019 [20]. The work function of the cathode electrode (Pt) stands at 5.65eV [21], facilitating its role as the back contact for hole transport. The defect layer parameters for the absorber layer, between ETL/$CH_3NH_3SnI_3$), and $CH_3NH_3SnI_3$/Graphene [18], The simulations were conducted within a voltage range scanning from 0V to 1.1V.

II. Results and discussion

2.1.: Initial Device Simulation

An initial device simulation was carried out for a CH3NH3SnI3 based device in the planar electron intrinsic hole(nip) configuration with Graphene as HTL, CdS as ETL's with Platinum having 5.65eV metal work function at the metal/ HTL interface. This configuration achieved an open-circuit voltage (Voc) of 0.9286V, represents the maximum voltage across the terminals of the solar cell when no current is flowing. This value indicates the efficiency of charge separation and the minimization of recombination processes within the cell. The short-circuit current density (Jsc) of 31.6897mA/cm², denotes the maximum current density generated when the voltage across the cell is zero (short-circuited condition). This value indicates the cell's ability to generate a substantial current under illumination. The fill factor (FF) of 77.45%, represents how well the solar cell utilizes the available power. A higher FF suggests efficient charge extraction and lower losses within the cell. The power conversion efficiency (PCE) of 22.79%, indicates the overall efficiency of the solar cell in converting incident light into electrical energy. This PCE value suggests a relatively high conversion efficiency for the tin-based perovskite solar cell.

2.2. Effect of varying the ETM Thickness

The thickness ETM's on the PSC was varied from 0.005µm to 0.0400µm, it was noted that the Voc and Jsc increases slightly with increasing ETM thickness, going from 0.928515V to 0.928592V and 31.68433(mA/cm²) to 31.69346 (mA/cm²). This is due to the fact that a thicker ETM can provide a more efficient pathway for electron transport. The energy level alignment at the ETM/perovskite interface can influence charge extraction and recombination [22]. A thicker ETM layer might lead to a better alignment of energy levels, reducing energy barriers for electron transport and potentially minimizing losses due to recombination, thus increasing the Voc and improving the overall current flow. The FF is seen to increase from 77.40% to 77.49% as the ETM thickness increases from 0.005µm to 0.0400µm. The increase in FF indicates improved charge extraction and reduced resistive losses within the solar cell structure. The overall efficiency is a function of the increased Voc, Jsc, and FF, which reached an optimal value of 22.81% at 0.04 µm. Figure (2) below shows the graphs of PV parameters as a function of ETM thickness.

2.3. Effect of varying the Absorber layer Thickness

A thicker absorber layer allows for greater light absorption due to the increased path length for photons within the perovskite material, [23]. A thicker absorber layer can absorb more photons and generate more electron-hole pairs [24]. This may have resulted in an increase in all the device parameters. The absorber layer thickness is varied from 0.600 to 0.950. This results in a higher Voc, as there is a greater potential difference between the electron-rich and hole-rich regions within the PSC. Short-Circuit current density (Jsc) is seen to increase significantly from 30.72689 (mA/cm²) to 32.45283 (mA/cm²). However, an optimal absorber thickness at 0.950µm with a FF of 77.95% is achieved. This is due to reduced resistive losses with increasing absorber layer thickness within the range of study. The optimal absorber layer thickness also depends on the wavelength of light and the optical properties of the perovskite material. The optimal absorber thickness within the range of study is seen at 0.95µm with a PCE of 23.67%. Fig. (3) below shows the graphs of the device parameters and the J-V curves.

2.4. Effect of varying the Bandgap energy of HTM

A bandgap with the right energy level alignment can help improve Voc by reducing energy losses through recombination at the interface [25]. It can influence the charge carrier mobility and concentration within the HTM, which, in turn, affects the current generation. The spectrum of incoming light, and the charge transport

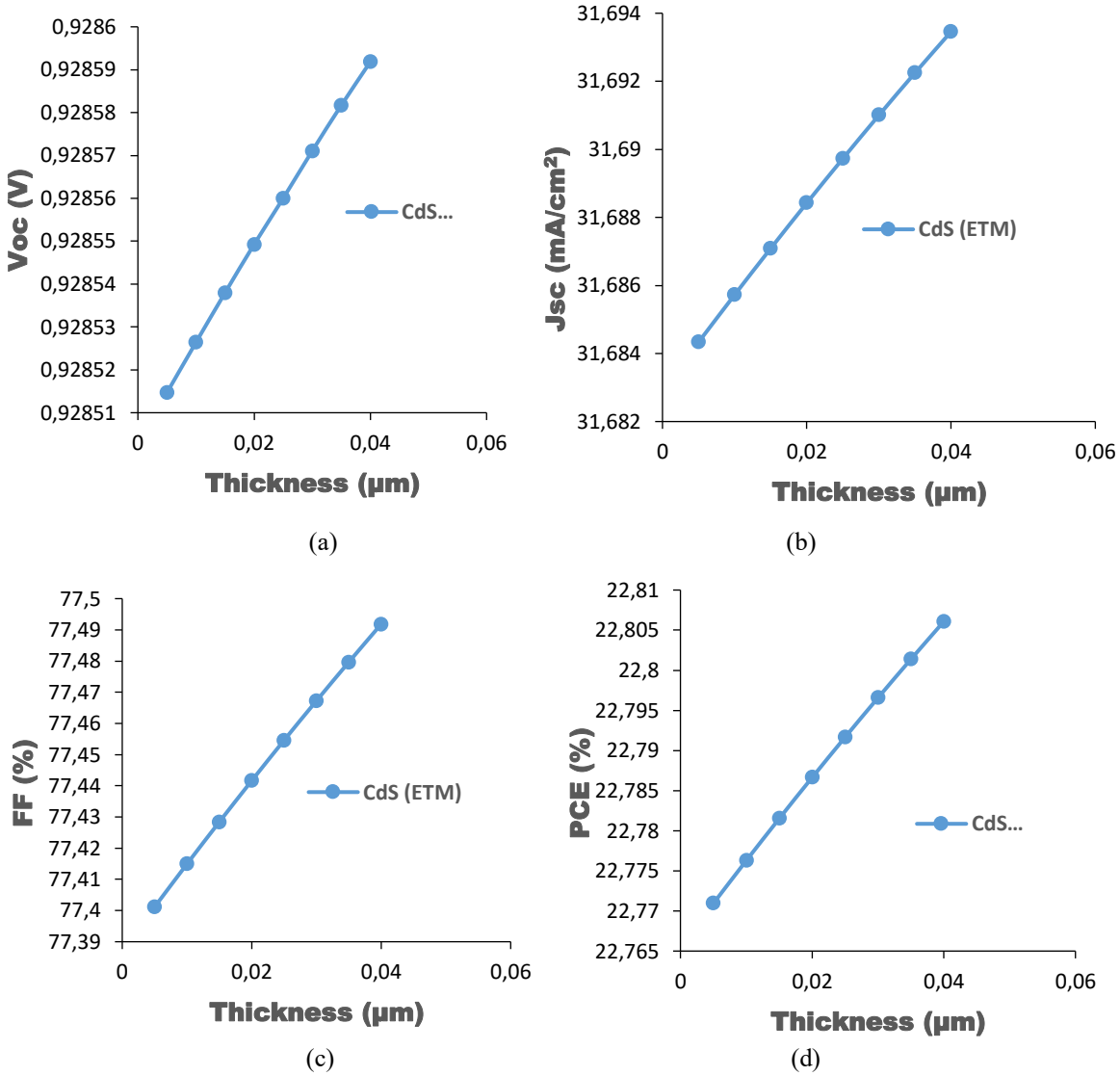

Fig. 2. (a), (b),(c),(d): Photovoltaic parameters as a function of ETM layer thickness.

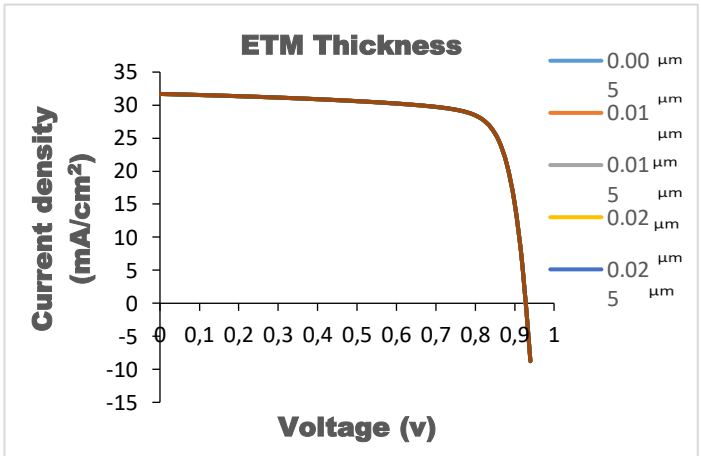

Fig. 2. (e) J-V curves as a function of ETM thickness.

mechanisms influence recombination processes [26], and careful tuning of these properties can lead to an improved fill factor and overall device efficiency. In this study the energy of the Bandgap is varied from 0.2 eV to 0.9 eV. This results in an increase in the Voc from 0.782587V to 0.960022V because higher bandgap reduces the thermalization losses. Higher bandgap materials can also generate higher voltage because they have a lower rate of non-radiative recombination, resulting in less energy loss as heat. It is also noted that higher bandgap materials absorb a larger portion of the solar spectrum, leading to increased current generation which resulted in the Jsc

increasing from 31.41 (mA/cm²) to 32.96(mA/cm²). The FF increased from 75.03% to 80.32% as the bandgap increases from 0.2 to 0.9 eV. The increase in FF indicates improved charge extraction and reduced resistive losses within the solar cell structure. It was observed that the efficiency increased from 18.45% to 25.41%. The increase in efficiency indicates that the higher bandgap HTM allows for better utilization of the incident solar radiation. Figure (4) below shows the graphs of PV parameters as a function of Bandgap energy.

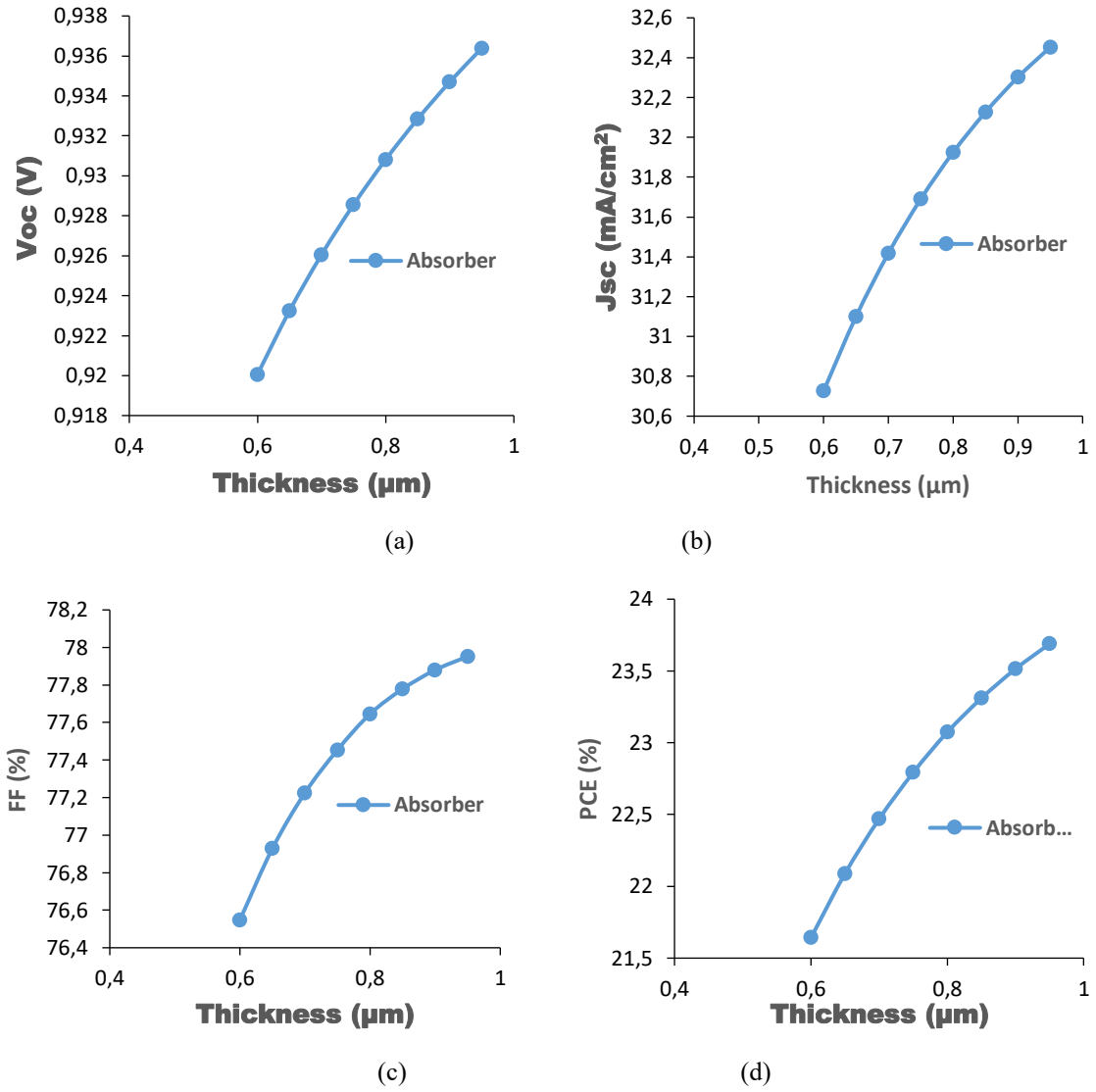

Fig. 3. (a), (b),(c),(d): Photovoltaic parameters as a function of Absorber layer thickness.

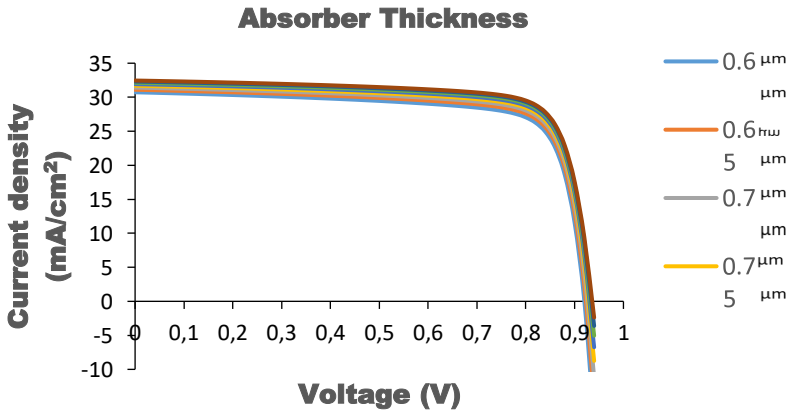

Fig. 3 (e). J-V Curves as a function of Absorber layer thickness.

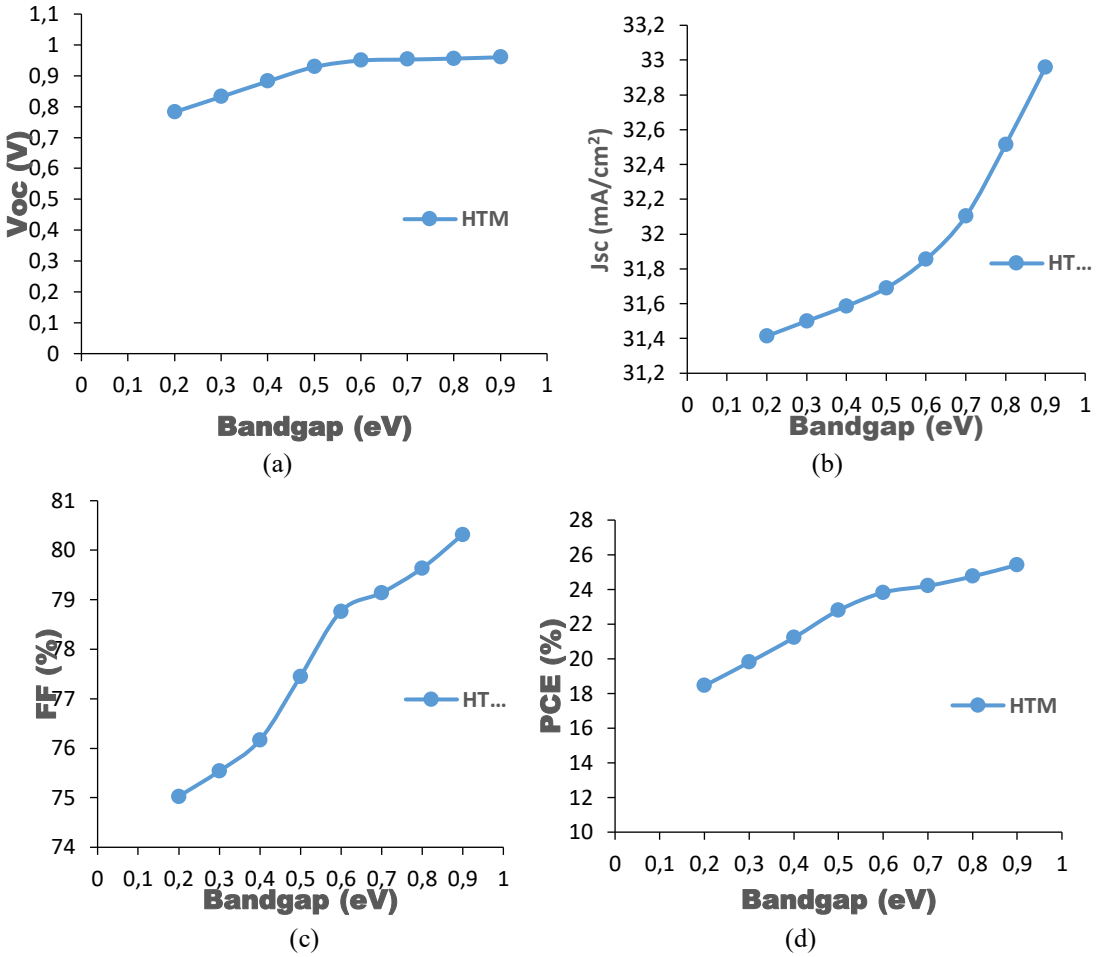

Fig. 4. (a), (b),(c),(d): Photovoltaic parameters as a function of Bandgap energy of HTM.

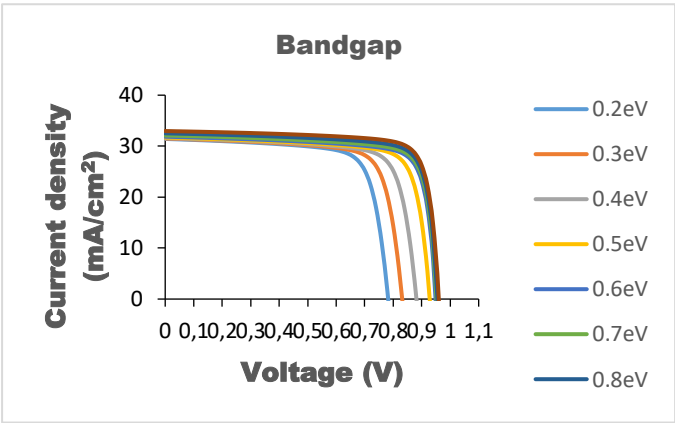

Fig. 4. (e) J-V Curves as a function of Bandgap energy of HTM.

2.5. Effect of Temperature variation on device performance of PSC

The open-circuit voltage (Voc) of the photovoltaic cell exhibits a slight decline from 0.9570V to 0.8429V with rising temperature. This phenomenon can be elucidated by the augmented energy levels of electrons within the valence band, consequently diminishing the potential disparity between the electrodes. Conversely, the short-circuit current density (Jsc) demonstrates minimal fluctuation, transitioning from 31.69 mA/cm² to 31.67 mA/cm² as temperature increases. This observation implies that the light absorption characteristics of the material remain largely unaffected within the temperature range under consideration. However, the mobility of charge carriers, encompassing electrons and holes, may attenuate with escalating temperature. This diminished mobility translates to slower movement of carriers within the device, thereby diminishing the overall current Additionally, the fill factor (FF) experiences a marginal decline from 77.31% to 76.69% with increasing temperature.

This reduction indicates a less efficient conversion of electrical power at elevated temperatures, attributable to augmented resistive losses within the device, along with alterations in charge carrier mobility and recombination dynamics. Interestingly, the FF initially witnesses a slight

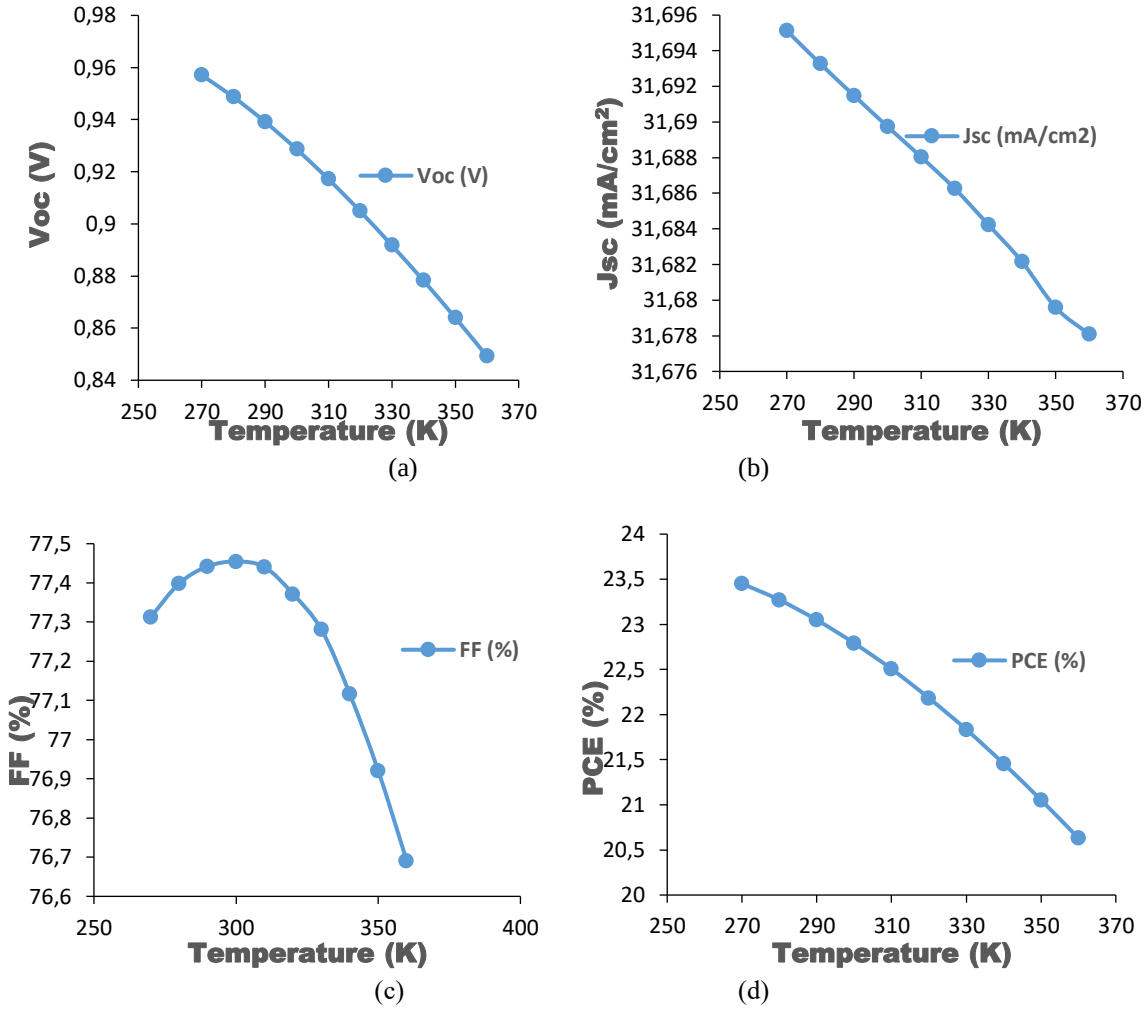

Fig. 5. (a), (b), (c), (d): Photovoltaic parameters as a function of Temperature variation.

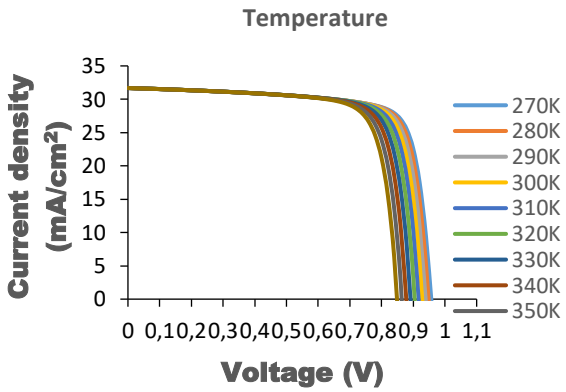

Fig. 5(e). J-V Curves as a function of Temperature variation.

augmentation, reaching 77.45% at 300K before subsequently declining to 76.69% at 360K. This fluctuation underscores the complex interplay of temperature and efficiency within the photovoltaic system. Furthermore, the power conversion efficiency (PCE) of the photovoltaic cell gradually diminishes from 23.45% to 20.63% with increasing temperature. This decline in efficiency can be ascribed to several factors, including reduced carrier mobility, heightened recombination rates, and altered charge transport properties at elevated temperatures. Additionally, thermal expansion may cause a reduction in the bandgap of the perovskite material, leading to decreased light absorption and, consequently, lower efficiency. Figure 5 below illustrates the graphical representation of the photovoltaic parameters as they vary with changes in temperature.

Conclusion

A tin-based ($CH_3NH_3SnI_3$) perovskite solar cell has been designed and constructed using SCAPS. Different

device parameters along with the working conditions of the device have been exclusively studied. According to the obtained simulation results, the ETM and absorber layer thickness was a crucial factor for the performance of the device. Increasing the ETM layer was optimal at 40nm. An absorber layer thickness of 950 nm was optimal for delivering a promising efficiency the impact of the bandgap variation of the hole transport material on the performance of the proposed solar cell structures have been investigated with optimal values of cell parameters at 0.9eV. The present study proposed a planar device architecture

Glass/FTO/CdS/$CH_3NH_3SnI_3$/Graphene/Pt for tin-based perovskite solar cells and it can also be utilized to investigate the effect of device parameters on other perovskite based solar cells. The final optimized device in this simulation obtained a PCE, Voc, Jsc and FF were 25.65%, 0.9606 V, 33.2491 (mA/cm^2), and 80.32% respectively Further, extensive experimental studies are required for the investigation of the proposed tin-based perovskite solar cell in order to completely replace the lead-based analogues since lead toxicity is a serious threat to our eco system.

Acknowledgements

We acknowledge Dr. Marc Burgelman, University of Gent, Belgium, for providing the free access to SCAPS-1D.

Owolabi J Adeyemi – PhD in Physics;
Ali H. – PhD in Physics;
Ijeoma N Ukorah – MSc in Physics;
Onimisi M.Y. – PhD in Physics;
Tafida R.A. – PhD in Physics;
Awujoola J Olalekan – PhD in Physics;
Gambo Hassan – MSc in Physics.

[1] International Renewable Energy Agency (IRENA). (2020). *Global Renewables Outlook: Energy transformation 2050*; https://www.irena.org/publications/2020/Apr/Global-Renewables-Outlook-2020.
[2] International Energy Agency (IEA). (2021). *Renewables 2021: Analysis and forecast to 2026*; https://www.iea.org/reports/renewables-2021.
[3] N.S. Lewis, *Research opportunities to advance solar energy utilization*. Science, 351(6271), aad1920 (2016); https://doi.org/10.1126/science.aad1920.
[4] Kiran Ranahat, Lee Patriteev, Alexandra Reevina, Kirill Andrianov, Valery Lapshinsky, Elena Sofrovova, *An introduction to solar cell technology*,14(4), 481 (2016); https://doi.org/10.5937/jaes14-10879.
[5] M. Raugei, P. Fullana-i-Palmer, & V. Fthenakis, *The energy return on energy investment (EROI) of photovoltaics: Methodology and comparisons with fossil fuel life cycles*. Energy Policy, 45, 576 (2012); https://doi.org/10.1016/j.enpol.2012.03.008.
[6] H. Li, J. Lin, X. Guan, X. Zhao, K. Yao, & Y. Liu, *Solar energy: Market penetration and potential in China.* Renewable and Sustainable Energy Reviews, 58, 750 (2016).
[7] S. Atamturktur, N. Karali, & V. Vittal, *Review of modeling tools for microgrid planning and design.* Renewable and Sustainable Energy Reviews, 56, 309 (2016);
[8] B.K. Sovacool, & M.H. Dworkin, Global energy justice: Problems, principles, and practices. Cambridge University Press. (2015).
[9] Y. Gan, Y. Qiu, Y. Zhao, C. Li, & X. Zhang, *Perovskite solar cells: Materials, structures, and performance*. Solar Energy Materials and Solar Cells, 240, 111442 (2022).
[10] G.Tong, S. Li, & L. Li, *Tin-Based Perovskite Solar Cells: Progress, Challenges, and Perspectives.* Solar RRL, 73(8), 1900049 (2019).
[11] M. Saliba, T. Matsui, K. Domanski, J.Y. Seo, A. Ummadisingu, S.M. Zakeeruddin, ... & M. Grätzel, *Incorporation of rubidium cations into perovskite solar cells improves photovoltaic performance*. Science, 354(6309), 206 (2016); https://doi.org/10.1126/science.aah5557.
[12] A. Kojima, K. Teshima, Y. Shirai, & T. Miyasaka, *Organometal halide perovskite solar cells*, The Journal of the American Chemical Society, 131(17), 6050-6051 (2009).
[13] Y. Wu, H. Chen, J. Wang, & H. Zhang, *Perovskite solar cells: Progress, challenges, and future perspectives*, Nano Energy, 84, 105841 (2021).
[14] L. Mai, Z. Liu, X. Wang, & W. Zhang, *High-efficiency perovskite solar cells: Recent advances and future challenges*, Advanced Materials, 34(22), 2107963 (2022).
[15] G.E. Eperon, G.M. Paternò, R.J. Sutton, A. Zampetti, A.A. Haghighirad, F. Cacialli, & H.J. Snaith, *Inorganic caesium lead iodide perovskite solar cells*. Journal of Materials Chemistry A, 3(39), 19688 (2015); https://doi.org/10.1039/C5TA06398A.
[16] M. Burgelman, P. Nollet, and S. Degrave, *Modelling polycrystalline semiconductor solar cells*, Thin Solid Films, 361-362, 527 (2000); https://doi.org/10.1016/S0040-6090(99)00825-1.
[17] M. Burgelman, D. Koen, N. Alex, V. Johan, and D. Stefaan, SCAPS manual (2014).
[18] A Md. Islam, N Md Bin Alamgir, S.I. Chowdhury, S.M.B. Billah, *Lead-free organic-inorganic halide perovskite solar cell with over 30% efficiency.* Article journal of ovonic research 18(3), 395 (2022), https://doi.org/10.15251/JOR.2022.183.395.

[19] S.H. Zyoud, A.H. Zyoud, A. Abdelkader, & N.M. Ahmed, *Numerical Simulation for Optimization of ZnTe-Based Thin-Film Heterojunction Solar Cells with Different Metal Chalcogenide Buffer Layers Replacements: SCAPS-1D Simulation Program*. International Review on Modelling and Simulations (I.RE.MO.S.), 14(2), 79 (2021); https://doi.org/10.15866/iremos.v14i2.19954.

[20] M. Gagandeep Singh, and R. Kumar, *Simulation of perovskite solar cell with graphene as hole transporting material*, in AIP Conference Proceedings, 2115 (1), 030548 (2019); https://doi.org/10.1063/1.5113387.

[21] T.J. Drummond, Work Functions of the transition Metals and Metal Silicides, article, February 15, (1999); Albuquerque, New Mexico. (https://digital.library.unt.edu/ark:/67531/metadc681130/m1/21/: accessedJuly 1, 2023).

[22] M. Liu, S. Pathak, T. Stergiopoulos, & H.J. Snaith, *Metallic electrodes for efficient perovskite solar cells*. Nature Energy, 1(6), 16056 (2016).

[23] W. S. Yang, J.H. Noh, N.J. Jeon, Y.C. Kim, S. Ryu, J. Seo, ... & S.I. Seok, *High-performance photovoltaic perovskite layers fabricated through intramolecular exchange.* Science, 348(6240), 1234. (2015); https://doi.org/10.1126/science.aaa9272.

[24] M. Liu, M.B. Johnston, & H.J. Snaith, *Efficient planar heterojunction perovskite solar cells by vapour deposition.* Nature, 501(7467), 395 (2013); https://doi.org/10.1038/nature12509.

[25] Z. Song,, S.C. Watthage, A.B. Phillips, R.J. Ellingson, & M.J. Heben, *Impact of halide composition on the electronic structure, optical properties, and solar cell performance of mixed-halide perovskites*. The Journal of Physical Chemistry C, 122(12), 6662 (2018).

[26] G.E. Eperon, V.M. Burlakov, P. Docampo, A. Goriely, & H.J. Snaith, *Morphological control for high performance, solution-processed planar heterojunction perovskite solar cells.* Advanced Functional Materials, 24(1), 151 (2014); https://doi.org/10.1002/adfm.201302090.

А.Дж. Оуволабі, Х. Алі[1], У.Н. Іджеома[1], М.Й. Онімісі[1], Р.А. Тафіда[1],
Дж. Олалекан Аувуджула[2], Х. Гамбо[1]

Дослідження ефективності сонячних елементів перовскітів на основі олова із сульфідом кадмію як etm та графеном як htm за допомогою SCAPS-1D

[1]*Кафедра фізики, Академія оборони Нігерії, Кадуна, Нігерія, jaowolabi@nda.edu.ng*
[2] *Директорат інформаційно-комунікаційних технологій NDA Кадуна, Кадуна, Нігерія*

Безсвинцеві сонячні елементи на основі перовскіту демонструють високий потенціал для відновлюваної енергії. Програмне забезпечення для моделювання SCAPS-1D використовувалося для моделювання пристрою безсвинцевого перовскітного сонячного елемента з архітектурою Glass/FTO/CdS/$CH_3NH_3SnI_3$/Graphene/Pt. Для оцінки продуктивності проведено процес оптимізації різних параметрів, таких як товщина ETM, поглинача, енергія забороненої зони матеріалу для транспорту дірок. Виконано обговорення їх впливу на параметри сонячної батареї. Оптимальна товщина шару ETM і матеріалу поглинача була досягнута при 40 нм і 950 нм. Енергія забороненої зони забезпечила оптимальну продуктивність параметрів пристрою при 0,9 еВ. Змодельовано зміни температури та відзначено, що кінцевий пристрій демонструє мінімальне зниження продуктивності параметрів PSC зі збільшенням температури. Остаточна оптимізована структура пристрою досягла PCE, Voc, Jsc і FF 25,65%, 0,9606 В, 33,2491 (мА/см^2) і 80,32% відповідно. Тому, очікується, що отримані висновки прокладуть шлях для розробки безсвинцевих і високоефективних перовскітних сонячних батарей.

Ключові слова: дірки; електрони; SCAPS-1D.